Electrochimica Acta 55 (2010) 8908–8915

Contents lists available at ScienceDirect

Electrochimica Acta

journal homepage: www.elsevier.com/locate/electacta

Studies of stoichiometry of electrochemically grown CdSe deposits

Krzysztof Bieńkowski, Marcin Strawski, Bartosz Maranowski, Marek Szklarczyk*

Laboratory of Electrochemistry, Department of Chemistry, Warsaw University, ul. Pasteura 1, 02-093 Warsaw, Poland

ARTICLE INFO

Article history:
Received 5 May 2010
Received in revised form 5 August 2010
Accepted 5 August 2010
Available online 14 August 2010

Keywords:
Cadmium selenide
Deposition
Stoichiometric ratio
Cyclic voltammetry
EDS
XRD

ABSTRACT

The proper deposition bath composition for electrochemical synthesis of the CdSe deposit in the hexagonal structure of the right elemental stoichiometry, and photoreacting as an n-type semiconductor which can be used as a stable photoanode is investigated. The deposits were prepared by a cyclic potentiodynamic technique and the concentration of Cd^{2+} and $SeO_3{}^{2-}$ in the deposition baths varied from 10^{-4} M to 0.1 M, and from 10^{-5} M to 10^{-3} M, respectively. The electrochemical, the X-ray diffraction (EDS and XRD), and the photoactivity studies of a number of deposits have shown that application of the solution composition following Cd:Se = 5:1 results in deposition of the stoichiometric CdSe. The detected ratio of reagents is explained on the base of reaction mechanism and necessary excess of cadmium ions preventing CdSe deposit dissolution. The procedure of CdSe electrosynthesis was developed to yield of a direct semiconductor in the hexagonal structure. The necessity for cadmium cations excess is explained on the basis of the mixed electrochemical/chemical deposition mechanism.

1. Introduction

Photoelectrochemistry started with Becquerel's studies on the photoeffects of solar illumination on metal electrodes in 1839 [1]. Much later it was understood that the most pronounced photoeffects were to be expected for semiconductive materials, while Brattain and Garrett observed large photocurrents during exposing a semiconductor electrode to the action of light of energy exceeding the electrode material band gap [2]. In the next years, photoelectrochemistry advanced rapidly [3–7]. The possibility of practical application of semiconductor electrodes was discussed by Williams as early as in 1960 [8]. A spark that ignited rapid research in electrochemistry of semiconductors was the observation of Fujishima and Honda [9,10]. These authors discovered a water photosplitting process at the irradiated TiO_2 electrode. The expectation for inexpensive production of hydrogen fuel resulted in an enormous increase in research effort in photoelectrochemistry field, which was additionally emphasised by the world oil crises (*e.g.* Refs. [11–17]). With time, because of some difficulties (*e.g.* low efficiency of photogalvanic cells) the interest in electrochemistry of semiconductors dropped significantly. A new attempt to develop these fields (electrochemistry of semiconductors and photoelectrochemistry) started with Brus's [18] demonstration that a quantum confinement of photocreated electron–hole pairs led to size dependent optical properties of semiconductor materials [19,20]. It drove the quest for the ways of preparation of nanostructured semiconductive materials, which exhibit new electronic and optical properties. But most attention was drawn to the synthesis of II–VI semiconductive nanocrystals and nanofilms, and among them cadmium selenide (CdSe) still remains one of the most thoroughly studied nanocrystal systems.

The CdSe band gap for bulk material is 1.7 eV, a threshold wavelength 729 nm [21], and depending on nanostructure radius, it might be tuned toward higher energy values (blue shift) up to 2.8 eV, a threshold wavelength 420 nm, for 1.2 nm nanocrystal [22]. Additionally, CdSe is a direct type of semiconductor and its electron affinity is in the range of 3.8–4.7 eV depending on nanostructure radius [23]. CdSe, because of its photoelectrochemical and photophysical properties is well known as a compound semiconductor suitable for solar energy conversion, optoelectronic devices, and for the preparation of antivirial drugs. It may also have a positive impact on the environment, as it was shown that it might be used to sequester CO_2 [24].

Methods for CdSe preparation can be divided into two major groups: dry methods carried out in the gas phase (vacuum evaporation and chemical vapor deposition) and wet methods (liquid phase synthesis and electrochemical deposition). While the gas phase techniques offer a high controllability of the growth of the structures and the feasibility to obtain a pure material, they, without exceptions, require an expensive high vacuum and high temperature equipment, and additionally, the gaseous waste material is another serious problem of these techniques.

The wet methods of CdSe nanostructures production are relatively inexpensive and simple to be carried out. Among a variety of the wet techniques, the electrochemical ones are the only

---

* Corresponding author. Tel.: +48 22 822 0211; fax: +48 22 822 5996.
E-mail address: szklarcz@chem.uw.edu.pl (M. Szklarczyk).

0013-4686/$ – see front matter © 2010 Published by Elsevier Ltd.
doi:10.1016/j.electacta.2010.08.024

techniques which can be used for a deposition of films on large and irregular surfaces. In comparison with other wet methods during electrodeposition, a strict control of an oxidation state of selenium is not required, the deposition occurs closer to an equilibrium state, and because the process is electrical in nature, it can be controlled precisely.

On the other hand, the electrochemical methods require a precise definition of experimental conditions such as potentials, reactant concentration, supporting electrolyte, deposition time, and the material of the working electrode is of great importance as well. The discussion on the theoretical thermodynamic conditions to be met to achieve cathodic deposition of stable binary semiconductor II–VI compounds have been developed by Kröger [25]. He distinguished two classes of deposition taking into account the difference in the deposition potential, the differences in the rate constants and exchange currents of the individual components. On this basis he tried to predict the stability of the deposits in dependence of the ions concentration in the bulk of the solution, and has found it to be proportional. Finally, he formulated the relations for the rest potentials in dependence on a discharge rate constant and ionic concentration. The deposition of CdSe he ascribed to class I, which means that this deposition is determined by a less noble selenium.

In previous years the CdSe was electrodeposited from the solutions of pH = 0 to pH = 14 [26–31]. The use of the reagent concentrations and their ratios varied widely, the Cd:Se ratio varied from 200:1 to 1:200 [26,29,31,32]. The potentials studied ranged from −1.5 V to 2.0 V [26,30]. The substrates used were Au, Pt, Ag, Cu, amalgamated Au [26,33], Ti [34], ITO [35] and HOPG [31]. A wide range of studied experimental conditions was examined in order to determine the best way of electrosynthesis of the material with the proper elemental stoichiometric ratio and of the suitable dimensions. Recently an excellent review on electrodeposition of semiconductive materials has been published by Lincot [36]. In this paper the two steps synthesis of semiconductive films is discussed, as well as the method of obtaining the precursor layer and after deposition annealing treatment. The influence of the deposition conditions on the free energy of the deposit formation is shown as an essential factor for the quality of the deposits.

The aim of the present studies was to investigate the influence of deposition solution composition on the elemental stoichiometry and photoreactivity of the CdSe surface structures. The deposits were prepared by a potentiodynamic technique, the concentration of Cd^{2+} varied from 0.1 M to 0.2 M, and the concentration of $SeO_3{}^{2-}$ varied from 10^{-5} M to 10^{-3} M. The elemental stoichiometry, compound formation and crystal structures were analyzed by X-ray energy dispersive spectroscopy (EDS) and X-ray diffraction spectroscopy (XRD), respectively. The photoelectrochemical activity of the CdSe structures was determined and the magnitude and direction of photocurrents were correlated with a structure and elemental stoichiometry.

2. Experimental

2.1. Electrodes and experimental procedures

A three-electrode and a three-compartment electrochemical cell with a quartz window were used. Working electrodes were made of a polycrystalline platinum disk. The working area was circular in shape, ca. 9 mm in diameter. The surface of the electrode was polished with alumina, down to 0.05 μm, and then it was cleaned with Millipore-Q water in an ultrasonic bath.

Counter electrodes were made of Pt/Pt gauze or wire, and an electrode potential was measured against an Hg|$HgSO_4$ reference electrode placed in saturated Na_2SO_4 solution. The potential values were recalculated to a normal hydrogen electrode scale (NHE) through this paper. Both counter and reference electrodes were placed in the compartments separated by a glass frit.

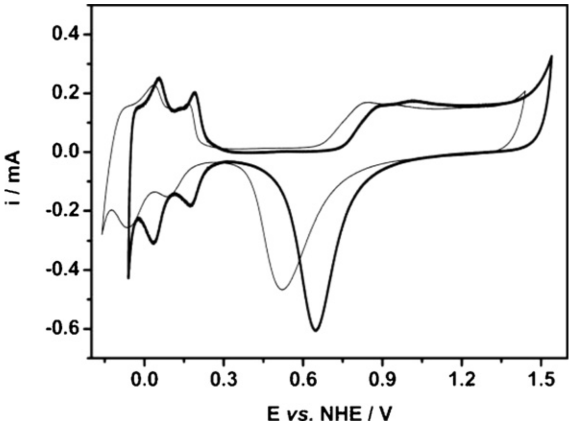

Fig. 1. The CV dependencies of the Pt electrode placed in 0.5 M H_2SO_4 solution (thick line) and 0.1 M Na_2SO_4 solution, (thin line). Sweep rate 50 mV s^{-1}.

Electrochemical activity of the working electrode surface and the purity of the solutions were checked by a cyclic voltammetry (CV), at first in an acidic solution (Fig. 1, thick line), and then in the solution of pH = 3 (Fig. 1, thin line). Obtaining of well defined CV dependencies for the Pt electrode attesting a measure of solution high quality was a desirable condition to start deposition experiments. CdSe deposition was carried out by a CV technique. The deposition time was determined by a number of CV cycles registered at 50 mV s^{-1}. A synthesized CdSe deposit was examined for its photoactivity by registering a CV dependence in the basic electrolyte solution free of Cd^{2+} and $SeO_3{}^{2-}$ ions. For the study of stoichiometry of the deposits the electrode was taken out of the cell, carefully washed out with Millipore-Q water, then dried and placed in a chamber of a secondary electron microscope (SEM) equipped with EDS device. The confirmation of the CdSe compound formation and detection of its crystallographic structure was done by an X-ray diffraction technique. In order to keep the electrode material constant, the XRD experiments were carried out for the CdSe deposits electrosynthesized on platinum substrate, which introduced a high background due to much higher absorption of X-ray energy by platinum than by graphite, which is usually employed as a substrate in such studies.

During the experiment, solutions were deoxygenated by bubbling Ar through an electrochemical cell and all experiments were carried out at an ambient temperature of 22 ± 2 °C.

2.2. Solutions

All solutions were prepared from Millipore-Q water and reagent grade $3CdSO_4{\cdot}8H_2O$, SeO_2, Na_2SO_4, and 98% H_2SO_4. The supporting electrolyte solution, pH = 3, was prepared from 0.5 M Na_2SO_4 solution, and pH was adjusted with 0.5 M sulfuric acid. The deposition baths (B) of five different Cd:Se ratios, 200:1 (BA), 5:1 (BB), 2:1 (BC), 1:1 (BD), and 1:5 (BE) were prepared by mixing $CdSO_4$ solution with SeO_2 solution. The Cd^{2+} concentration range varied from 10^{-4} M to 0.1 M, while $SeO_3{}^{2-}$ concentration varied from 10^{-5} M to 10^{-3} M. The composition of the deposition baths is given in Table 1.

2.3. Equipment

A three-electrode cell with a quartz window was used in all experiments. The current–voltage behavior was monitored with a programmed potentiostat (EG&G 263A, U.S.A.).

Table 1
Chemical composition of deposition baths.

No.	Solution composition	Cd:Se ratio in the bulk of solution
BA1	2×10^{-3} M Cd^{2+} + 10^{-5} M $SeO_3{}^{2-}$	200:1
BA2	2×10^{-1} M Cd^{2+} + 10^{-3} M $SeO_3{}^{2-}$	
BB1	5×10^{-4} M Cd^{2+} + 10^{-4} M $SeO_3{}^{2-}$	5:1
BB2	5×10^{-3} M Cd^{2+} + 10^{-3} M $SeO_3{}^{2-}$	
BC2	2×10^{-4} M Cd^{2+} + 10^{-4} M $SeO_3{}^{2-}$	2:1
BC2	2×10^{-3} M Cd^{2+} + 10^{-3} M $SeO_3{}^{2-}$	
BD1	1×10^{-4} M Cd^{2+} + 10^{-4} M $SeO_3{}^{2-}$	1:1
BD2	1×10^{-3} M Cd^{2+} + 10^{-3} M $SeO_3{}^{2-}$	
BE1	10^{-4} M Cd^{2+} + 5×10^{-4} M $SeO_3{}^{2-}$	1:5
BE2	10^{-3} M Cd^{2+} + 5×10^{-3} M $SeO_3{}^{2-}$	

The source of light was a 1 kW xenon lamp placed in a lamp housing (LSH 521, LOT ORIEL, Germany). A water filter was placed between the cell and the source of light to filter out the long-wavelength part of radiation in order to avoid excessive heating of the solution.

SEM imaging was done with a LEO 435 VP microscope (Germany). The device used a low sample current to give the highest possible resolution and a detailed structure imaging. Under such conditions, the effect of charging up was diminished. The chamber pressure was 10^{-6} Torr and pictures were registered for 7 keV or 15 keV electron beam energy to obtain the best quality images. The samples prior to being placed in vacuum, were washed out with Millipore-Q water and then dried.

Elemental analysis measurements were carried out with multichannel EDS device (Röntec, model M1, Germany). The pressure in the chamber was 10^{-6} Torr. EDS spectra were measured at 15 keV electron beam energy. For each sample four places of the diameter ca. 1 mm^2 were studied and in the paper the average of these measurements is quoted.

The XRD analysis was carried out with an X-ray diffractometer (Bruker D8 Discover). The radiation source was Cu Kα, λ = 1.5406 Å. Measurements were done in a sample free orientation mode, and the total acquisition time was 15,000 s.

3. Results and discussion

3.1. Electrochemistry of Cd^{2+} + $SeO_3{}^{2-}$ solution

The CV dependence for Pt electrode placed in BB2 solution registered for the wide potential range, −1.0 to 1.5 V, is presented in Fig. 2A. Two CV runs are presented, the initial run followed by the steady state run. Various peaks and plateaus can be distinguished. To assign these features it is necessary to take into account the deposition and dissolution of CdSe itself and additionally the possible redox processes of Cd^{2+} and $SeO_3{}^{2-}$ ions. Furthermore, because the general goal is to produce either nano/micro structures or thin films, it is always possible that some parts of the working electrode material free of deposit is exposured to the solution, and its electroactivity can also be observed. The most important reactions are listed in Table 2. The strong dependence of the reaction potential on electrode material and solution composition can easily be noted. Such a situation can easily result in misleading reaction identification on the basis of the shape of CV dependence, and correct process classification requires cautious approach.

The dependencies presented in Fig. 2A were started to be registered in the cathodic direction from ca. 0.1 V. After five cycles a steady-state curve was registered (Fig. 2A, thick line). During the first cycle (Fig. 2A, thin line) C4–C7 features were distinguished. The C4 and C5 maxima are likely to represent cadmium under potential deposition (UPD), reaction 3, Table 2, because at the beginning of the first cycle the Pt electrode surface is still free of any deposits and this potential range is rather too anodic for selenium ions reduction or CdSe depositon. The following peak, C6, can be ascribed to two processes, *i.e.* cadmium bulk deposition and a CdSe formation, reactions 1 and 17, Table 2. The shift of this peak with cycling can be explained by the decreasing energy of CdSe formation on the surface covered with some Cd/CdSe even if the film is not continuous. Such a deposit might be considered as a nucleation center for further deposition. The current increase above −0.88 V we ascribe to the onset of hydrogen evolution reaction. On the anodic side, in the first run, the peak at ca. −0.42 V, A1, is due mainly to the Cd oxidation process (reaction 2, Table 2) and possibly to the CdSe dissolution (reaction 18, Table 2). Two well pronounced maxima at 0.87 V, A3, and 1.23 V, A4, can be attributed to the oxidation of selenium to selenite (reaction 12 Table 2), and to the oxidation of CdSe to selenite, respectively (reaction 19, Table 2).

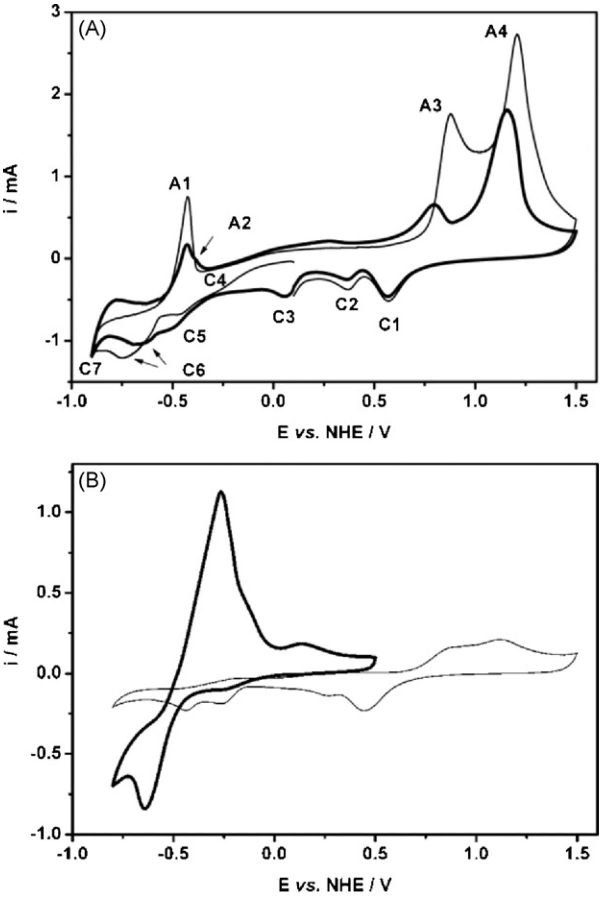

Fig. 2. The CV dependencies of the Pt electrode placed in: (A) 5×10^{-3} M $CdSO_4$ + 10^{-3} M SeO_2 + 0.1 M Na_2SO_4 solution, pH = 3. First and steady state runs are denoted by thin and thick lines, respectively. Sweep rate 50 mV s^{-1}; (B) thick solid line was registered for 5×10^{-3} M $CdSO_4$ + 0.1 M Na_2SO_4 solution, pH = 3; thin solid line was registered for 10^{-3} M SeO_2 + 0.1 M Na_2SO_4 solution, pH = 3.

Going cathodic, the peaks at 0.55 V, C1, and 0.35 V, C2, are formed. Viewing the potential values they do not correspond to any reactions in Table 2. To identify these processes, it is necessary to compare the CV dependencies presented in Fig. 2A with those presented for the supporting electrolyte solution in Fig. 1, solid line, and a CV dependence for this solution but registered over wider potential range (Fig. 3). On both figures a cathodic peak at ca. 0.55 V is observed. This peak is due to the desorption of adsorbed oxygen layer from the Pt electrode surface. An additional argument for identification of C1 peak, Fig. 2A as an oxygen desorption process is a current magnitude of this maxima. In all cases (Fig. 1, solid line,

Table 2
The list of reactions and observed potentials at electrodes placed in solutions containing Cd^{2+} or/and SeO_3^{2-} ions.

No	Reaction	Potential (V)	Conditions	Refs
1	$Cd^{2+} + 2e^- \rightarrow Cd$	Onset at −0.88	CdSe single crystal electrode in 0.1 M Na_2SO_3, pH = 7, SCE	[27]
		Onset at −0.75	Ti electrode with CdSe deposited film, 0.25 M $CdSO_4$, pH = 2.5, SCE	[29]
		−0.75	Ag electrode covered with Se, 1 mM $CdSO_4$, pH = 8.5, Ag/AgCl	[30]
2	$Cd \rightarrow Cd^{2+} + 2e^-$	−0.48	Ti electrode covered with CdSe deposited film, 0.25 M $CdSO_4$, pH = 2.5, SCE	[29]
		−0.76	HOPG, 0.08 M $CdSO_4$, pH = 3, SCE	[31]
3	$Cd^{2+} + e^- \rightarrow Cd^+ + e^- \rightarrow Cd$ (UPD process)	−0.41 to −0.69	Ag electrode covered with Se, 1 mM $CdSO_4$, pH = 8.5, Ag/AgCl	[30]
4	$SeO_3^{2-} + 8H^+ + 6e^- \rightarrow H_2Se + 3H_2O$	−0.38	HOPG, 2×10^{-3} M SeO_2, pH = 3, SCE	[31]
		−0.5	Au electrode, 0.5 mM Na_2SeO_3 + 0.1 M $CdSO_4$ + 0.25 M Na_2SO_4, pH = 0, SCE	[26]
5	$SeO_3^{2-} + 6H^+ + 6e^- \rightarrow Se^{2-} + 3H_2O$	−1.05	Au electrode, 0.1 M $(NH_4)_2SeO_3$ + 2.15 M $(NH_4)_2SO_3$ + 4.5 M NH_3, EDTA, pH = 9.4, SCE	[37]
6	$H_2SeO_3 + Cd^{2+} + 4H^+ + 6e^- \rightarrow CdSe + 3H_2O$	Onset at −0.6	HOPG electrode, 0.8 mM H_2SeO_3 + 0.08 M $CdSO_4$, pH = 3, SCE	[31]
7	$HSeO_3^- + 6H^+ + 6e^- \rightarrow HSe^- + 3H_2O$	0.29	Pt electrode, 0.5 mM SeO_2 + 0.1 M $NaClO_4$, SCE	[38]
8	$SeO_3^{2-} + 6H^+ + 4e^- \rightarrow Se + 3H_2O$	−0.45	Ti electrode covered with CdSe deposited film, 0.25 mM H_2SeO_3 + 0.25 M $CdSO_4$, pH = 2.5, SCE	[29]
9	$Se^{4+} + 4e^- \rightarrow Se$	Onset at −0.6	Ag electrode, 0.5 mM Se (IV), pH = 8.5	[30]
10	$Se + 2e^- \rightarrow Se^{2-}$	−0.92	Ti electrode, 0.01 M H_2SeO_3 + 1 M K_2SO_4, pH = 2.4, NHE	[32]
		−1.0	Ti electrode covered with CdSe deposited film, 0.25 mM H_2SeO_3 + 0.25 M Na_2SO_4, pH = 2.5, SCE	[29]
		Onset at −1.1	CdSe single crystal electrode, 0.1 M Na_2SO_3 solution, pH = 7, SCE	[27]
11	$Se + H^+ + 2e^- \rightarrow HSe^-$	−0.51	Ti electrode, 0.01 M H_2SeO_3 + 1 M K_2SO_4, pH = 2.4, NHE	[32]
12	$Se + 3H_2O \rightarrow H_2SeO_3 + 4H^+ + 4e^-$	0.8	HOPG electrode, 1 mM H_2SeO_3 + 0.12 M $CdSO_4$, pH = 2.7, SCE	[31]
13	$Se^{2-} + 3H_2O \rightarrow SeO_3^{2-} + 6H^+ + 6e^-$	−0.65	Au electrode,0.1 M $(NH_4)_2SeO_3$ + 2.15 M $(NH_4)_2SO_3$ + 4.5 M NH_3, EDTA pH = 9.4, SCE	[37]
14	$H_2Se \rightarrow Se + 2H^+ + 2e^-$	−0.74	Au electrode, pH = 0, SCE	[26]
15	$HSe^- + PtO + H^+ \rightarrow PtSe + H_2O$	0.2	Pt electrode, 0.24 mM H_2SeO_3 + 0.1 M H_2SO_4, SCE	[39]
16	$Cd^{2+} + Se^{2-} \rightarrow CdSe$	Onset at −0.65	Au electrode, 0.1 M $(NH_4)_2SeO_3$ + 2.15 M $(NH_4)_2SO_3$ + 4.5 M NH_3, EDTA, pH = 9.4, SCE	[37]
17	$Cd^{2+} + SeO_3^{2-} + 6H^+ + 6e^- \rightarrow CdSe + 3H_2O$	Onset at −0.72	Ti electrode covered with CdSe deposited film, 0.25 mM H_2SeO_3 + 0.25 M $CdSO_4$ + 0.25 M Na_2SO_4, pH = 2.5, SCE	[29]
18	$CdSe \rightarrow Cd^{2+} + Se^{2-}$	−0.25	Au electrode, 0.1 M $(NH_4)_2SeO_3$ + 2.15 M $(NH_4)_2SO_3$ + 4.5 M NH_3, EDTA pH = 9.4, SCE	[37]
		−0.50	Ti electrode covered with CdSe deposited film, 0.25 mM H_2SeO_3 + 0.25 M $CdSO_4$ + 0.25 M Na_2SO_4, pH = 2.5, SCE	[29]
19	$CdSe + 3H_2O \rightarrow Cd^{2+} + H_2SeO_3 + Cd^{2+} + 4H^+ + 6e^-$	1.3	HOPG electrode, 1 mM H_2SeO_3 + 0.12 M $CdSO_4$, pH = 2.7, SCE	[31]

Fig. 2A and Fig. 3) its magnitude is almost the same, 0.5 mA. A similar explanation was proposed by Šimkūnaitė et al. [40]. The second cathodic peak, 0.35 V (C2, Fig. 2A) can be recognized on the basis of similar analysis as a peak due to the hydrogen adsorption process, which is represented in Fig. 1, and Fig. 3 by a cathodic current in the potential range 0.0–0.25 V. The weak point of such an explanation is that the potential of this peak is too anodic and the potential difference between peaks C1 and C2, Fig. 2A, is only 0.22 V while in Fig. 3 it is ca. 0.4 V. An alternative to hydrogen adsorption could be either reaction 4 or 9 (Table 2), for which the potentials reported [30,31] are fairly close. The third explanation for the appearance of this maximum could be a formation of the surface selenide, PtSe in agreement with reactions 7 and 15 [38,39].

There are few differences between the peak spectrum observed in the first CV cycle and in the subsequent ones (Fig. 2A). The peak at 0.05 V, C3, followed by a plateau up to −0.4 V can be attributed to reaction 8, Table 2, *i.e.* to the selenium deposition reaction. Some authors identify this potential range as the sum of 8, 10, 16 reactions [41]. Another important difference is the anodic shift of the C6 peak. It can be explained by a decrease in the energy of the Cd^{2+} reduction and CdSe formation on the existing Cd/CdSe film in comparison to the Pt electrode surface. A similar explanation can

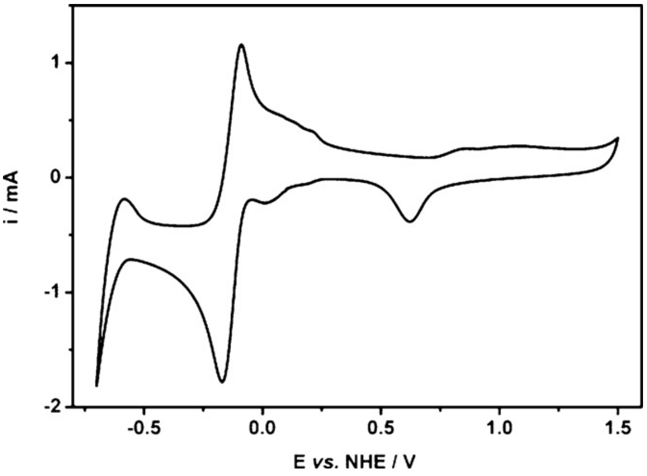

Fig. 3. The CV dependency of the Pt electrode placed in 0.1 M Na_2SO_4 solution, pH = 3. Sweep rate 50 mV s^{-1}.

be applied to the anodic shifts of A3 and A4 peaks. An interesting feature is the formation of the plateau, A2, on the anodic side of the A1 peak. We ascribe this phenomenon to the splitting cadmium (A1) oxidation from the dissolution of the CdSe film (A2). It has to be noted that the electrode potentials of the reactions proposed above differ in some cases from those listed in Table 2. We explain these discrepancies as the differences in the electrochemical activity of the electrode material surface. Platinum is known for being one of the most electroactive electrode materials, especially towards adsorption of different species. These exclusive properties of platinum might be the explanation for the reaction potential differences between potentials observed in this work and those listed in Table 2, especially A3, A4, C5, C6 that show the lower energy reaction at Pt electrode.

Two cathodic, −0.2 V, −0.7 V, and two anodic maxima, −0.65 V, −0.15 V are detected (Fig. 3) in a cathodic potential range, both are not detected in the solution containing Cd^{2+} and ${SeO_3}^{2-}$ ions (Fig. 2A). The proposed explanation for this observation has to take into account the process of the reduction of the supporting electrolyte, because there is nothing else in this solution. We propose that following hydrogen adsorption the evolution starts at −0.05 V, but then the current decreases because reduction of sulfates and adsorption of the product of this reaction take place at such a negative potential. The adsorbed product blocks the hydrogen evolution process. The further cathodic change of the electrode potential results in a hydrogen evolution below −0.7 V on the new electrode surface. The anodic peak at −0.65 V is probably due to a hydrogen desorption, and the peak observed at −0.15 V is due to the oxidation of adsorption layer.

For comparison the CV dependencies for Pt electrode placed in either Cd^{2+} (thick solid line) or ${SeO_3}^{2-}$ (thin solid line) solutions for the same concentration as that in the mixture (Fig. 2A), are shown in Fig. 2B. Note that the CV dependence for the mixture of both ions (dotted line) is not an over imposition of the individual dependencies. Some differences in the peak potentials and current magnitude are easily seen. The current due to Cd^{2+} reduction and Cd deposit oxidation strongly decreases in the mixture of the ions (*cf.* Fig. 2B thick solid line and Fig. 2A thin solid line), while the currents in the potential range where the Se and CdSe deposit oxidation take place are much larger than those registered in the mixture of the ions (*cf.* Fig. 2B thin solid line and Fig. 2A thin solid line). As expected the anodic peak A1, Fig. 2A, due to the cadmium oxidation is much larger in the pure solution of Cd^{2+} cations. The potential peak A3 (Fig. 2A), which was identified as reaction 12 (Table 2) in the absence of Cd^{2+} cations in the bulk of solution, disappeared. The potential plateau observed above 0.76 V might be ascribed to the platinum surface oxide formation. The potential peak at 1.13 V observed for ${SeO_3}^{2-}$ solution, Fig. 2B, thin solid line, cannot be ascribed to the oxidation of CdSe as it was identified as peak A4 in Fig. 2A. This maximum is proposed here to be identified with the oxidation of Se deposit to H_2SeO_3 process, *i.e.* reaction 12, Table 2. It means that this process is shifted anodically by ca. 0.3 V in comparison with its potential in the ion mixture solution (peak A3, Fig. 2A). Apparently the energy of oxidation of Se co-deposited with CdSe is lower than that of pure Se deposit and can indicate the occurrence of catalytic properties of CdSe towards Se oxidation.

The main differences in the cathodic branches of the CV dependencies registered either in the mixture of ions (Fig. 2A thin solid line) or in ${SeO_3}^{2-}$ solution (Fig. 2B, thin solid line) are the absence of the C3 potential peak in ${SeO_3}^{2-}$ solution, and the occurrence of two new peaks at −0.26 V and −0.43 V in this solution. The absence of the C3 potential peak in ${SeO_3}^{2-}$ solution indicates that the identification of this process proposed above as the sum of reactions 8, 10 and 16, Table 2 is false and that this peak can be ascribed to reaction 16 alone. The new peaks at −0.26 V and −0.43 V (Fig. 2B, thin solid line) can be ascribed to the formation of Se deposit (reaction 8, Table 2) and then its reduction to HSe^- anion (reaction 11, Table 2).

3.2. *Influence of solution composition on CdSe stoichiometry and its photoactivity*

On the basis of the studies of Cd^{2+} + ${SeO_3}^{2-}$ solution electrochemistry the potential range 0.4 V to −0.9 V was chosen for the studies of the CdSe deposit preparation. The CV curves are presented in Fig. 4A–E. The first observation is that for the baths BA (Cd:Se ratio 200:1), BD (Cd:Se ratio 5:1), BC (Cd:Se ratio 2:1) the maxima for CdSe and Cd deposition are well defined, while for the bath BD (Cd:Se ratio 1:1) it is not the case, and the oxidation peak for CdSe/Cd is not observed, which indicates that the deposit is either extremely thin, it is in an island form, or it is not formed at all. For BD2 baths, *i.e.* for a higher concentration, 10^{-3} M, it starts to manifest itself slightly. This comparison confirms the idea that the Cd:Se ratio in the bulk solution might be much more important for the deposit formation and its stoichiometry than the magnitude of the concentration itself.

The examples of SEM image of CdSe deposit and EDS spectrum (insert) are presented in Fig. 5. The SEM picture shows that electrosynthesized deposit is in an dendrite island form. The EDS spectrum was obtained by focusing an X-ray beam on the CdSe structures (white species in Fig. 5).

In order to check if these structures are the CdSe in the chemical compound form rather than the elemental mixture, a XRD technique was employed and a typical result is presented in Fig. 6. The corresponding line spectra for Pt, CdSe in cubic (zinc blende) form and CdSe in hexagonal (wurzite) form provided by the JCPDS (Joint Committee on Powder Diffraction Standards) are presented in this figure. As expected, the CdSe signal is strongly overlaid by the Pt signals. Independently of this difficulty, clear signals for the CdSe can be distinguished in the presented diffraction pattern, in the angular region between 23° and 30°, at 42°, 49.8°, and 71.8°. The complex maximum between 23° and 30° indicates the presence of a wurzite structure, but the single maximum at 49.8° indicates a zinc blende structure. For the hexagonal structure a triplet maximum (2 0 0, 1 1 2, 2 0 1 peaks) is expected [42] around this angle, but since the 1 1 2 peak is much more pronounced in most cases than the two sides peaks, the presence of the single peak can be considered as the signal from the hexagonal structure, too [43,44]. The peak at 42° can be tied up with either a cubic or a hexagonal structure, but the peak at 71.8° is ascribed only to a hexagonal structure. It has to be stressed that the wurzite form of CdSe was

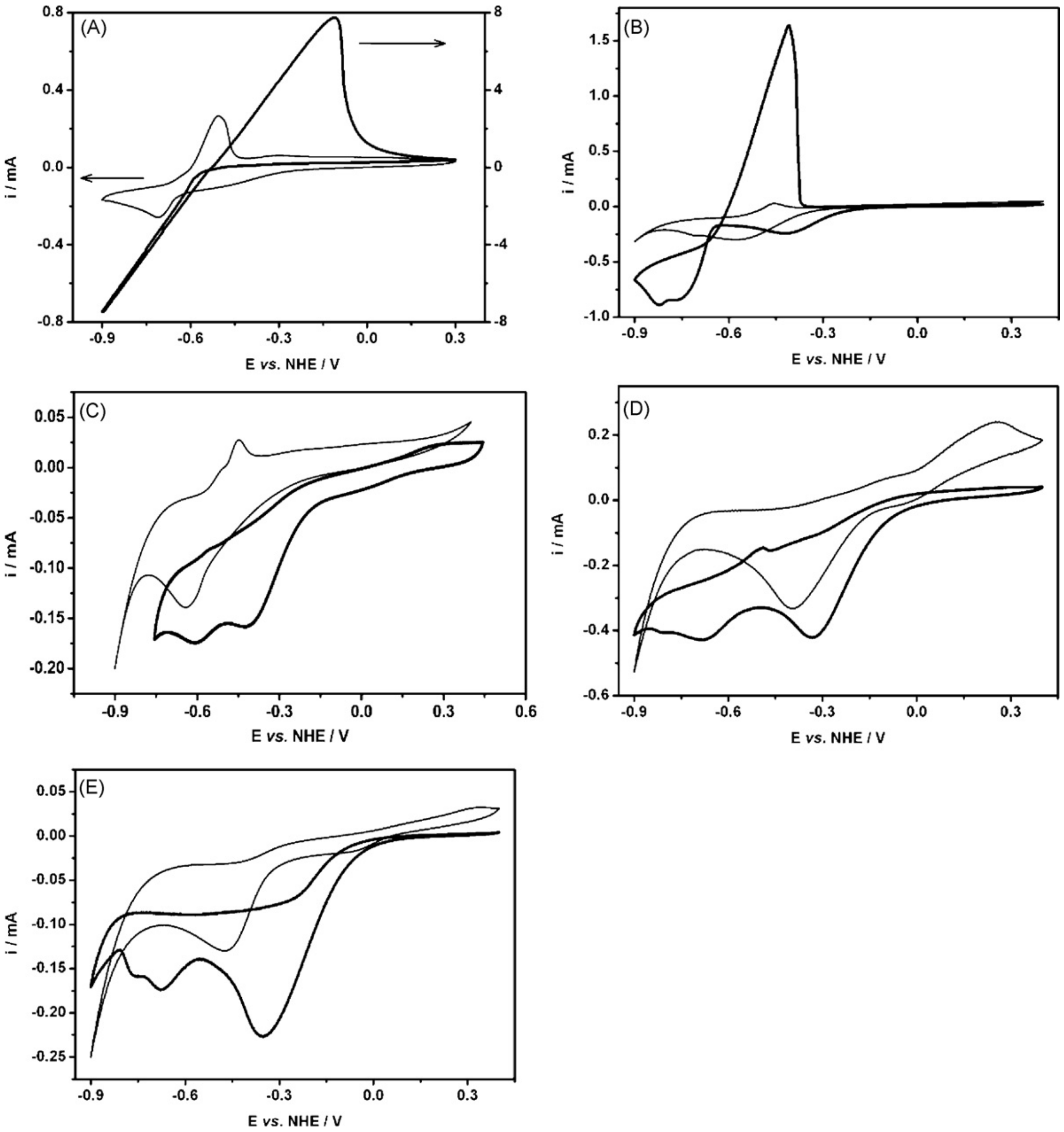

Fig. 4. The CV dependencies of the Pt electrode placed in: (A) BA1 and BA2 solutions denoted by thin and thick lines, respectively; (B) BB1 and BB2 solutions denoted by thin and thick lines, respectively; (C) BC1 and BC2 solutions denoted by thin and thick lines, respectively; (D) BD1 and BD2 solutions denoted by thin and thick lines, respectively; and (E) BE1 and BE2 solutions denoted by thin and thick lines, respectively. pH = 3. Sweep rate 50 mV s^{-1}.

obtained with no use of the thermal treatment often necessary for transformation of the cubic into hexagonal form [42]. Summarizing the XRD data, one may state that the hexagonal form of CdSe was deposited, but the inclusions of a cubic form are probably present, as well.

The EDS analysis results are given in Table 3. The EDS data were obtained only for the more concentrated solution at a given Cd:Se ratio, because for the lower concentration the deposit was not massive enough to obtain a signal intensity that could be analyzed. From the data presented in Table 3 it is clear that with the decreasing Cd:Se ratio in the bulk of solution the elemental Cd:Se ratio decreases, and below the ratio of 5:1 the Se amount in deposit dramatically increases. The stoichiometric deposits were obtained for the high Cd:Se ratios in the bulk of the solution. Similar results

Table 3
Elemental composition of deposits obtained by EDS technique.

Bath	Solution composition	Cd:Se ratio in the bulk of solution	Cd:Se ratio in deposit
BA2	10^{-1} M Cd^{2+} + 10^{-3} M $SeO_3{}^{2-}$	200:1	1:13
BB2	5×10^{-3} M Cd^{2+} + 10^{-3} M $SeO_3{}^{2-}$	5:1	1:1
BC2	2×10^{-3} M Cd^{2+} + 10^{-3} M $SeO_3{}^{2-}$	2:1	1:1.9
BD2	10^{-3} M Cd^{2+} + 10^{-3} M $SeO_3{}^{2-}$	1:1	1:3
BE2	10^{-3} M Cd^{2+} + 5×10^{-3} M $SeO_3{}^{2-}$	1:5	0:1

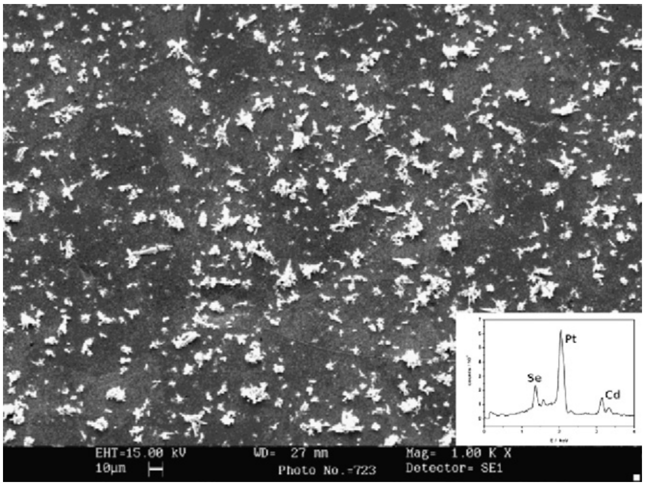

Fig. 5. The images of CdSe deposits taken by SEM technique. The insert is an EDS spectrum registered exclusively for the structure observed. The deposit was obtained from BB2 solution. The electrode was taken out of the solution after five cycles between −0.9 V and 0.35 V. The white bar at the bottom represents 10 μm.

were obtained for Ti electrode [29,38], HOPG electrode [31] and Ni electrode [38].

To confirm the results obtained by EDS technique, which is a statistical method yielding the results strongly dependent on the place of the surface chosen for analysis, the photoactivity of the produced deposits was studied. The results are presented in Fig. 7. For the deposit obtained from the BB solution, for which the stoichiometric elemental ratio was detected as 1:1 (Table 3), the photocurrent observed is n-type (Fig. 7A) as expected for CdSe material. The second deposit tested was the one obtained from BC solution for which a small excess of selenium was observed (Table 3). In this case the decreasing n-type and increasing p-type photo response were observed (Fig. 7B), proving the presence of some Se for which the p-type response is expected. The time dependence of the photoeffect (Fig. 7B) indicates that the deposit obtained from the solution of the Cd:Se ratio equal to 2:1 is unstable, and decomposes to cadmium ion and selenium. For deposit obtained from BE solution a stable p-type photoeffect was detected (Fig. 7C) as it is expected

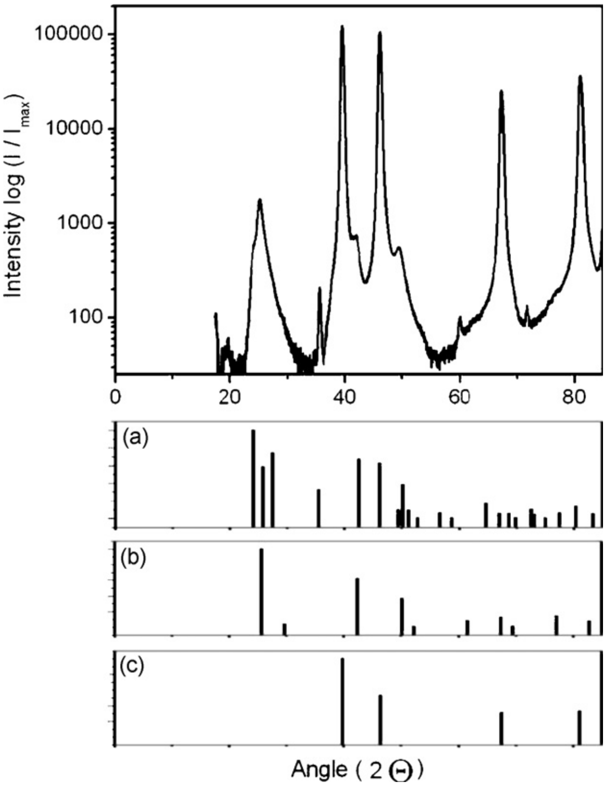

Fig. 6. XRD spectra. The uppermost spectrum was registered for CdSe deposit electrosynthesized on Pt electrode from BB2 solution. The line spectra are JCPDS reference. (a) CdSe spectrum in hexagonal (wurzite) form (spectrum number 75-5680), (b) CdSe in cubic (zinc blende) form (spectrum number 65-2891), and (c) Pt surface (spectrum number 65-2868).

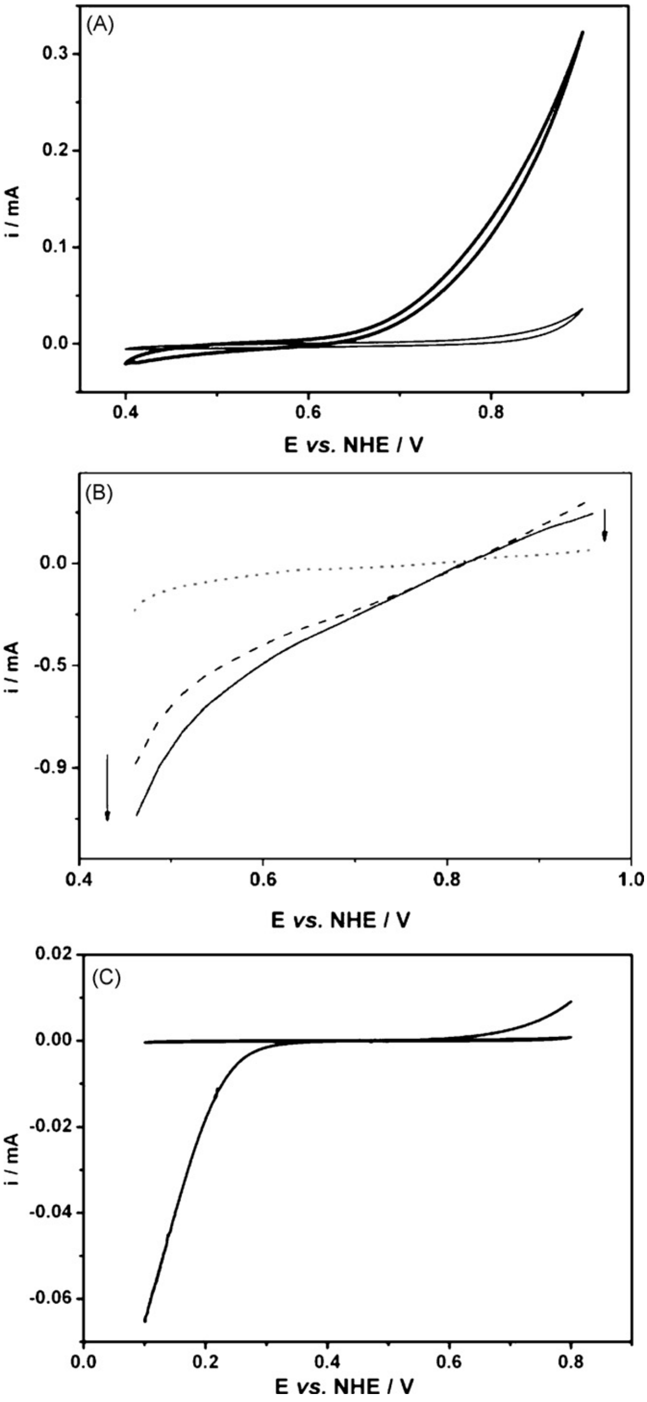

Fig. 7. The V–i_{ph} dependencies for CdSe deposit obtained from (A) BB1 solution, (B) BC2 solution and (C) BE2 solution. (A and C) Photo and dark currents are denoted by thin and thick lines, respectively. (B) The cathodic runs are shown. The dark current is denoted by dotted line, the first and the last photocurrent runs are denoted by dashed and solid lines respectively. Arrows point the direction of the change of the photocurrent with cycling. pH = 3. Sweep rate 50 mV s^{-1}.

for a pure selenium, and it is in agreement with the data presented in Table 3.

The determined requirement for the excess of Cd^{2+} concentration over $SeO_3{}^{2-}$ concentration for deposition of stoichiometric CdSe is in need of an explanation. The first and the most obvious explanation would be the lower transport rate of Cd^{2+} ions in comparison with the $SeO_3{}^{2-}$ transport rate. The diffusion coefficient for Cd^{2+} is reported to be in the range of $5.6–8.0 \times 10^{-6}\,cm^2\,s^{-1}$ [32,45], while for $SeO_3{}^{2-}$ it is ca. $5.6 \times 10^{-6}\,cm^2\,s^{-1}$ [32]. It is obvious that such a small difference in the ionic transport cannot be the reason for the ca. 5:1 excess of cadmium ions over selenite ions.

The possible explanation might be based on the reaction mechanism of the CdSe depositon. In the literature the proposition of different deposition reaction mechanisms might be found (for some review please check Ref. [46]). These mechanisms involve different number of cadmium cations.

The most often quoted mechanism [46] involves equal number of cadmium and selenium based ions;

$$H_2SeO_3{}^{2-} + 6H^+ + 6e^- \rightarrow H_2Se + 3H_2O$$

$$Cd^{2+} + H_2Se \rightarrow CdSe + 2H^+$$

A reaction requiring the highest number of cadmium cations was proposed by Tomkiewicz et al. [47] and it involves an initial reduction of cadmium ions followed by chemical oxidation of Cd by selenites;

$$3Cd^{2+} + 6e^- \rightarrow 3Cd$$

$$3Cd + SeO_3{}^{2-} + 6H^+ \rightarrow CdSe + 3H_2O + 2Cd^{2+}$$

The three cadmium cations requirement for one selenite anion in the above cited reactions is close to the concentration ratio detected in this work. Furthermore, some excess of Cd^{2+} cations in the solution is required to prevent CdSe dissolution [37]. The proposed deposition mechanism confirms Kröger's classification of the CdSe deposition as class I of the deposition processes of semiconductor film [25].

4. Conclusion

The bath composition is not the only parameter affecting the stoichiometry of electro-deposited films, but it is a fundamental one, which is pointed out in this work.

It has been shown here that the ratio $Cd^{2+}:SeO_3{}^{2-} = 5:1$ is the most satisfactory to obtain the deposit of the right elemental stoichiometry (Cd:Se = 1:1) and photoreacting as an n-type semiconductor. The detected ratio of reagents can be explained on the base of reaction mechanism involving three cadmium ions and necessary excess of cadmium ions preventing CdSe deposit dissolution.

The presented procedure of CdSe electrosynthesis leads to the deposition of direct semiconductor in the hexagonal structure. The necessity for cadmium cations excess results from the proposed mixed electrochemical/chemical deposition mechanism.

Acknowledgement

We are grateful to the Ministry of Education and Science for the support of this paper through grant program 3T08A 04128. We are very grateful to Dr Mikołaj Donten for his help in assistance during EDS measurements.

References

[1] E. Becquerel, C.R. Acad. Sci. 9 (1839) 561.
[2] W.M. Brattain, C.G.B. Garrett, Bell Syst. Tech. J. 34 (1955) 129.
[3] J.F. Dewald, in: B. Hannay (Ed.), Semiconductors, Reinhold, New York, 1957, p. 725.
[4] M. Green, in: J.O'M. Bockris (Ed.), Modern Aspects of Electrochemistry, vol. 2, Butterworths, London, 1959, p. 343.
[5] H. Gerischer, in: P. Delahay (Ed.), Advances in Electrochemistry and Electrochemical Engineering, vol. 1, Interscience, New York, 1961, p. 139.
[6] V.A. Myamlin, Y.V. Pleskov, Electrochemistry of Semiconductors, Nauka, Moscow, 1965.
[7] J. McHardy, F. Ludwig (Eds.), Electrochemistry of Semiconductors and Electronics; Processes and Devices, Noyes Publication, Park Ridge, 1992.
[8] R. Williams, J. Chem. Phys. 32 (1960) 1505.
[9] A. Fujishima, K. Honda, S. Kikuchi, J. Chem. Soc. Jpn. 72 (1969) 108.
[10] A. Fujishima, K. Honda, Nature 37 (1972) 238.
[11] Y. Nakato, S. Tonomura, H. Tsubomura, Ber. Bunsenges. Phys. Chem. 80 (1976) 1002.
[12] K. Ohashi, J. McCann, J.O'M. Bockris, Energy Res. Abstr. 1 (1977) 259.
[13] W. Kautek, J. Gobrecht, H. Gerischer, Ber. Bunsenges. Phys. Chem. 80 (1980) 1034.
[14] A. Heller, R.G. Vadimsky, Phys. Rev. Lett. 46 (1981) 1153.
[15] M.A. Butler, D.S. Ginley, 163rd Electrochem. Soc. Meet., San Francisco, 1983 (ext. abst. 773).
[16] M. Szklarczyk, J.O'M. Bockris, Appl. Phys. Lett. 42 (1983) 1035.
[17] E. Smotkin, A.J. Bard, A. Campion, M.A. Fox, T. Mallouk, S.E. Webber, J.M. White, J. Phys. Chem. 90 (1986) 4604.
[18] L.E. Brus, J. Chem. Phys. 80 (1984) 4403.
[19] L.E. Brus, J. Chem. Phys. 79 (1983) 5566.
[20] M.L. Steigerwald, L.E. Brus, Acc. Chem. Res. 23 (1990) 183.
[21] K. Rajeshwar, N.R. de Tacconi, C.R. Chenthamarakshan, Chem. Mater. 13 (2001) 2765.
[22] S.J. Rosenthal, J. McBride, S.J. Pennycook, L.C. Feldman, Surf. Sci. Rep. 62 (2007) 111.
[23] N.C. Greenham, X. Peng, A.P. Alivisatos, Phys. Rev. B 54 (1996) 17628.
[24] L.G. Wang, S.J. Pennycook, S.T. Pantelides, Phys. Rev. Lett. 89 (2002) 075506.
[25] F.A. Kröger, J. Electrochem. Soc. 125 (1978) 2028.
[26] M.S. Kazacos, B.J. Miller, Electrochem. Soc. 127 (1980) 869.
[27] R. Tenne, G. Hodes, Ber. Bunsenges. Phys. Chem. 89 (1985) 74.
[28] S.J. Lade, M.D. Uplane, C.D. Lokhande, Mater. Chem. Phys. 68 (2001) 36.
[29] C.M. Shen, X.G. Zhang, H.L. Li, Appl. Surf. Sci. 240 (2005) 34.
[30] F. Loglio, M. Innocenti, F. D'Acapito, R. Felici, G. Pezzatini, E. Salvetti, M.L. Foresti, J. Electroanal. Chem. 575 (2005) 161.
[31] Q. Li, M.A. Brown, J.C. Hemminger, R.M. Penner, Chem. Mater. 18 (2006) 3432.
[32] A. Lukinsas, I. Savickaja, V. Jasulaitienė, J. Juodkazytė, T. Juodiene, P. Kalinauskas, Chemija 13 (2002) 89.
[33] L.P. Colleti, B.H. Flowers, J.L. Stickney, J. Electrochem. Soc. 145 (1998) 1442.
[34] M. Bouroushian, Z. Loizos, N. Spyrellis, G. Maurin, Appl. Surf. Sci. 115 (1997) 103.
[35] T. Edamura, J. Muto, Thin Solid Films 226 (1993) 135.
[36] D. Lincot, Thin Solid Films 487 (2005) 40.
[37] St. Kutzmutz, G. Láng, K.E. Heusler, Electrochim. Acta 47 (2001) 955.
[38] R. Modolo, M. Traore, O. Vittori, Electrochim. Acta 31 (1986) 859.
[39] P. Carbonnelle, L. Lamberts, Electrochim. Acta 340 (1992) 53.
[40] D. Šimkūnaitė, E. Ivaškevič, V. Jasulaitienė, V. Steponavičius, Chemija 13 (2002) 219.
[41] A.M. Kressin, V.V. Doan, J.D. Klein, M. Sailor, J. Chem. Mater. 3 (1991) 1015.
[42] R.J. Bandaranayake, G.W. Wen, J.Y. Lin, H.X. Jiang, C.M. Sorensen, Appl. Phys. Lett. 67 (1995) 831.
[43] B.O. Dabbousi, J. Rodriguez-Viejo, F.V. Mikulec, J.R. Heine, H. Mattousii, R. Ober, K.F. Jensen, M.G. Bawendi, J. Phys. Chem. B 101 (1997) 9463.
[44] D.J. Peña, J.K.N. Mbindyo, A.J. Carado, T.E. Mallouk, C.D. Keating, B. Razawi, T.S. Mayer, J. Phys. Chem. B 106 (2002) 7458.
[45] S. Kariuki, H.D. Dewald, Electroanalysis 8 (1996) 307.
[46] R.K. Pandey, Handbook of Semiconductor Electrodeposition, first ed., CRC Press, 1996.
[47] M.T. Tomkiewicz, I. Ling, W.S. Parsons, J. Electrochem. Soc. 129 (1982) 2016.